NASA Technical Memorandum 79251

THE CHEMISTRY OF SODIUM CHLORIDE INVOLVEMENT IN PROCESSES RELATED TO HOT CORROSION

Carl. A. Stearns, Fred J. Kohl
and George C. Fryburg
Lewis Research Center
Cleveland, Ohio

Prepared for the
Conference on Advanced Materials for Alternate Fuel Capable Directly Fired Heat Engines
Castine, Maine, July 30-August 3, 1979

THE CHEMISTRY OF SODIUM CHLORIDE INVOLVEMENT IN PROCESSES RELATED TO HOT CORROSION

by Carl A. Stearns, Fred J. Kohl, and George C. Fryburg
NASA-Lewis Research Center
Cleveland, Ohio 44135

Sodium chloride is one of the primary contaminants that enter gas turbine engines and contribute, either directly or indirectly, to the hot corrosion degradation of hot-gas-path components. It has been difficult to define completely the role played by sodium chloride in the hot corrosion process because the fate of the ingested salt is complex. Various physical and chemical processes can take place as the salt proceeds through the compressor, combustor, and turbine. Some of the ingested salt is separated out of the air stream by the compressor. However, sodium chloride does pass from the compressor to the combustor where numerous chemical reactions can take place. Here some of the salt is vaporized to yield gaseous sodium chloride molecules; hydrogen and oxygen atoms present in the combustion products react with some sodium chloride to yield other gaseous species such as sodium; and a fraction of the salt remains as particulates. Both the gas phase and condensed sodium chloride can lead to sodium sulfate formation by various routes, all of which involve reaction with sulfur oxides and oxygen. It is of course well established that sodium sulfate is directly involved in the hot corrosion process. In addition to contributing to the formation of sodium sulfate, the sodium chloride can contribute to corrosion directly.

At the NASA-Lewis Research Center, we have been endeavoring to understand the chemistry of sodium chloride in the combustion process, in the deposition process, and in reactions with certain oxides on the surfaces of superalloys. Laboratory experiments together with thermodynamic and mass transport calculations have been used to elucidate the behavior of sodium chloride in combustion environments. This paper surveys the results obtained in the various Lewis in-house and contract- and grant-supported studies.

INTRODUCTION

Directly fired heat engines for propulsion and power generation systems require components that will function for long times at high temperatures and stresses in hostile environments. While these components are designed primarily on the basis of mechanical properties, in practice component life

is found increasingly often to be controlled by environmental attack. This situation is expected to intensify as the use of dirty alternate fuels becomes more prominent and the high temperature combustion environment becomes more hostile. This scenario has provided the impetus for the development of advanced materials that at elevated temperatures possess good mechanical properties together with inherent environmental resistance. To continue to make progress toward this objective requires an understanding of the mechanisms of fundamental processes involved in environmental attack.

In general, environmental attack arises from synergistic combination of (1) high temperatures, (2) combustion products of the air and fuel burned, and (3) impurities which enter the system with the air and/or fuel. Sodium chloride, NaCl, is one of the primary contaminants that enters the gas turbine engine and contributes to the degradation of hot-gas-path components. The role played by NaCl in the hot corrosion process has been difficult to define completely because (1) the fate of the ingested contaminant is complex and (2) there has been a lack of fundamental information on the various physical and chemical processes which take place as the NaCl proceeds through the gas turbine engine.

In the hot corrosion literature one can easily find a number of misconceptions about the role of NaCl in the hot corrosion process. We choose to itemize some of these as:

1. NaCl aerosol cannot be converted to NaCl(g) in the time available in a turbine engine hot section.
2. NaCl cannot be converted to Na_2SO_4 in the residence time of a gas turbine engine.
3. NaCl is completely converted to Na_2SO_4 in the presence of O_2 and SO_2.
4. NaCl reacts at high temperature and P_{O2} with Cr_2O_3(s) to transport chromium via the gaseous species Na_2CrO_4, $CrCl_3$ or CrO_2Cl_2.
5. NaCl is converted to Na_2SO_4(g) which condenses on components to yield and be the only source of the corrosive Na_2SO_4(1).

These misconceptions provided an initial stimulus for much of the research reported here. This paper is an overview of NASA-Lewis Research Center in-house and contract/grant supported programs directed toward obtaining an understanding of the chemistry of sodium chloride as related to processes involved in hot corrosion environmental attack. These studies have been concerned mainly with three areas: (1) the combustion process, (2) the deposition process, and (3) gas-solid interactions. While we shall consider specifics in the context of the gas turbine engine, much of the chemistry will apply to other systems which may involve closely related impurities. For example, coal fired systems are expected to experience high temperature corrosion problems resulting from release of alkali halide impurities in the coal. Likewise, MHD systems will have corrosion problems resulting from alkali sulfates formed in the system. The NASA studies have been of a

sufficiently fundamental nature that they also find application beyond the context of the gas turbine engine.

The chemistry of NaCl in the combustion process has been studied experimentally by mass spectrometric sampling of salt-and sulfur-doped laboratory flames (Ref. 1-3). Experimental results have been compared with equilibrium thermochemical calculations for the experimental gas compositions and conditions. Reactions between NaCl(c) and hydrogen or oxygen atoms have been examined in a NASA sponsored study (Ref. 4,5). Also, the deposition of sodium sulfate, Na_2SO_4, on cooled inert collectors has been studied in-house by seeding the combustor of a Mach 0.3 burner rig with NaCl or sea salt (Ref. 6). Experimental deposition rate results have been compared with the predictions of a multicomponent mass transfer theory developed under NASA grants (Ref. 7,8). The kinetics of conversion of NaCl(c) to Na_2SO_4(c) by reaction with O_2 and SO_2 is being examined in-house by thermogravimetric and mass spectral methods. Finally, gas-solid interaction studies have centered mainly on effects associated with exposure of alloys to low levels of gaseous NaCl. Target collection and mass spectrometric techniques have been employed to investigate the vapor transport of material away from oxide surfaces (Ref. 9,10). Thermogravimetry and microscopy were used to study the kinetics and surface morphology in gaseous NaCl - oxide surface interactions (Ref. 11-14).

SUMMARY OF NaCl INVOLVEMENT

It is useful at the start to examine the overall physicochemical behavior of NaCl ingested into a turbine engine. Figure 1 shows a conception of the fate of NaCl which can enter the system by a number of possible routes. Past studies (Ref. 15-18) have investigated physical aspects of NaCl containing aerosols as they pass through the various engine sections and these shall not be considered here. The important fact to note is that regardless of compressor separation etc., NaCl does ultimately enter the high temperature combustion region. Here, as depicted in Figure 1, some NaCl can be vaporized, some can undergo reaction with hydrogen and oxygen atoms produced early during combustion, and some of the NaCl may remain unchanged in both its physical and chemical state. The products of these three possible processes are NaCl(g), Na(g) and NaCl(c).

Gaseous NaCl can contribute directly to corrosion by gas-solid interactions or it can become involved in various gas-gas interactions to yield species such as NaOH(g), and Na_2SO_4(g). The Na(g) product can undergo gas-gas interactions to also contribute to the production of these species. Like the NaCl(g), the NaOH(g) and HCl(g) species can, by gas-solid interactions, effect corrosion directly or synergistically. The NaCl(c) that exits the combustor can undergo gas-solid interactions in the moving hot gas stream or the salt particles can impact on airfoil surfaces and undergo reactions on these hot surfaces. Either route leads to the formation of Na_2SO_4 deposits. Of course, condensation and vapor transport mass transfer processes also lead to the formation of highly corrosive Na_2SO_4(l) deposits.

In the conceptual scheme shown in Figure 1 the possibility has also been provided for some NaCl to pass through the hot section without becoming involved in the corrosion process. Obviously this overall conception is highly schematic and no quantitative aspects have been attached to the various routes. To obtain some insight into the quantitative aspects one must consider in detail the chemistry and kinetics of the various individual processes.

The following sections review the chemistry and kinetics. For in-depth details of the experimental methods and measured results the reader is referred to the respective references cited.

COMBUSTION CHEMISTRY

Until recently, there was considerable speculation regarding the molecular compostion of sodium-containing species in flames and the kinetics of the gas phase formation of sodium sulfate. Generally it had been assumed that sulfur impurities in the fuel and the sodium chloride impurity in the ingested air react during combustion to yield gaseous sodium sulfate by overall reactions of the type:

$$2\ NaCl(g) + SO_2(g) + 1/2\ O_2(g) + H_2O(g) = Na_2SO_4(g) + 2\ HCl(g) \qquad (1)$$

$$2\ NaOH(g) + SO_2(g) + 1/2\ O_2(g) = Na_2SO_4(g) + H_2O(g) \qquad (2)$$

A recent Lewis Research Center high temperature Knudsen cell investigation of the vaporization of sodium sulfate (Ref. 19) has lent credence to such reactions by establishing the existence of the $Na_2SO_4(g)$ molecule and by providing values for its thermodynamic properties (Ref. 20). To obtain a greater understanding of the chemistry and kinetics of hydrocarbon flames doped with sulfur and sodium salts, high pressure sampling mass spectrometry has been used to measure the composition of combustion products in several laboratory flames (Ref. 1-3). The experimental results were compared with equilibrium thermodynamic calculations of combustion gas composition.

Flame Compositions

Flame Sampling by Mass Spectrometry

Direct mass spectrometric analysis of the species present in salt and sulfur doped atmospheric pressure flames was accomplished with a high pressure, free-jet expansion, modulated molecular beam mass spectrometric sampler. A schematic diagram of the experimental arrangement is shown in Figure 2. This technique allows one to sample all the gas phase species directly while preserving their dynamic and chemical integrity (i.e., frozen chemistry). The theory and a description of the sampler have been presented elsewhere (Ref. 21). Premixed fuel-lean methane/oxygen flames were burned on a laminar flow, flat flame burner (Ref. 1-3). Sulfur was added to the gas mixtures as either SO_2 or CH_3SH. In addition, the gas mixtures could be seeded with alkali salts (e.g., NaCl or Na_2CO_3) by nebulizing aspirated water solutions into the mixing chamber of the burner. A typical flame had a luminous zone located somewhat less than one millimeter above the top

surface of the burner and a thickness of about one millimeter. The burner was supported by a mechanical device so that the vertical distance between burner and sampler, perpendicular to the flame front, could be varied. Composition profiles were obtained by measuring the various gaseous species as a function of distance from the burner surface (or residence time), through the flame and into the post-flame region.

Results are given in Figure 3 for a CH_4/O_2 flame doped with SO_2 and seeded with an aspirated solution of NaCl. The flame speed was 42 cm sec^{-1}. The most significant observations are (1) the gaseous Na_2SO_4 molecule was formed; (2) the residence time required for formation of $Na_2SO_4(g)$ was less than one millisecond; (3) not all of the NaCl was converted, that is, gaseous NaCl persists in the flame; (4) sodium- sulfur-containing intermediate species $NaSO_2(g)$ and $NaSO_3(g)$ were identified; and (5) the expected permanent gaseous products (e.g. CO_2, H_2O, etc.) were identified.

Calculations of Flame Composition

To facilitate a comparison of experimental observations with equilibrium thermodynamic predictions, the mole fractions of flame reaction products were calculated (Ref. 1-3). The calculations were made with the widely used NASA complex chemical equilibrium computer program (Ref. 22). This program is based on the minimization of free energy approach to chemical equilibrium calculations, subject to the constraint of maintaining a proper mass balance between reactants and products. The program permits calculation of chemical equilibrium compositions in homogeneous or heterogeneous systems for assigned thermodynamic states such as temperature-pressure (T,P) and enthalpy-pressure (H,P).

The role of NaCl in methane/oxygen flames was examined by obtaining flame temperatures and compostions as a function fuel/oxidant mass ratio. In the calculations, the convention used was that CH_4 and SO_2 were labeled fuel and O_2, H_2O, and NaCl were labeled oxidant. The calculated equilibrium compositions of the reacted flame gas products at the adiabatic flame temperatures are presented in Figure 4 as a function of fuel/oxidant ratio. The major products are in the first plot and the sodium-containing species are in the second. To arrive at the distribution of molecular species depicted in Figure 4, the program considered over 70 gaseous and condensed phase species made up of C-H-O-S-Na-Cl combinations. Note that only those molecular species for which the program was given thermodynamic data were considered in the calculations; no data for $NaSO_2$ or $NaSO_3$ are available.

The results of the calculations showed that the sodium is distributed in a complex pattern between $Na_2SO_4(c)$, NaCl(g), NaOH(g), $Na_2SO_4(g)$, Na(g), $NaCl_2(g)$, NaO(g), and NaH(g). At low values of the fuel/oxidant ratio (corresponding to low flame temperatures), and up to a sharp cut-off point, the sodium is tied up almost exclusively in the condensed phase as $Na_2SO_4(c)$. Based on the calculations, gaseous Na_2SO_4 can be expected to be present in significant amounts only over a relatively narrow fuel/oxidant ratio range and would always be present at a molar concentration of less than one-tenth that of NaCl(g). At high fuel/oxidant ratios, NaOH(g), Na(g), and NaCl(g) were found by our calculations to account for most of the sodium.

Experimental results shown in Figure 3 can be compared with the calculated results shown in Figure 4 by noting that, according to the fuel and oxidant convention used, the fuel/oxidant mass ratio for the experimental flame was 0.072. For ease of comparison, calculated mole fractions of product species for this ratio are shown on the right-hand side of Figure 3. At the outset one must recognize that the following two factors affect this comparison: (1) the experimental results were not "calibrated" for various mass spectrometric sensitivity factors and (2) the calculations are for equilibrium conditions only, at the adiabatic flame temperature. With these factors in mind, the agreement between experiment and calculation is considered to be good for all of the species except possibly NaCl and Na_2SO_4. Several reasons may account for the disagreement between experiment and calculations for these two particular species: (1) the sodium level in the flame has uncertainty associated with it due to the method used to introduce the sodium chloride; (2) the concentration of $Na_2SO_4(g)$ is a rapidly varying function of temperature and fuel/oxidant ratio; and (3) the true flame temperature is expected to be significantly below the calculated adiabatic flame temperature of 2032K. We have calculated that if the flame were 200K cooler, the predicted level of $Na_2SO_4(g)$ would equal the experimental level. By reflecting on all of the factors above, we concluded that the agreement between experiment and calculation is reasonably good for all species. Thus calculations can be useful in predicting, at least qualitatively, what is to be expected in experimental doped flame systems.

The $NaCl(g)/SO_2/H_2O/O_2$ Reaction

The reaction between gaseous NaCl, O_2, SO_2, and H_2O has been studied by mass spectrometrically sampling the gases from a reaction tube through which the mixture flowed (Ref. 1). The residence time in the reactor was about two seconds. The product species $Na_2SO_4(g)$, $SO_3(g)$, and $NaSO_3(g)$ were observed as illustrated in Figure 5. The relative concentrations of each species, including $Na_2SO_4(g)$ and $SO_3(g)$ compared well with those calculated by equilibrium thermodynamics. These measurements demonstrate that equilibrium is readily achieved in such a gas mixture at temperatures above 1000K.

Reactions of NaCl(c) with Hydrogen and Oxygen Atoms

It is generally believed that, in flames, NaCl(c) first vaporizes and its sodium is released via gas phase reactions between the resultant NaCl vapor and atomic hydrogen (Ref. 23). However, for large particles, the residence time in the combustor may be insufficient for complete vaporization (Ref. 17). Thus the possibility arises that heterogeneous reactions may contribute to sodium release. The kinetics of such reactions, or important rivals to them, have not previously been explored in any detail.

As part of a NASA-sponsored program to elucidate the basic kinetics and mechanisms of these processes, Professor D. E. Rosner and Dr. P. D. Foo at Yale University have been examining heterogeneous reactions between solid NaCl and atomic hydrogen or oxygen (Ref. 4,5):

$$H(g) + NaCl(s) \rightarrow Na(g) + HCl(g) \quad (3)$$

$$O(g) + NaCl(s) \rightarrow Na^*(g) + ClO(g) \quad (4)$$

Here the asterisk represents the excited state of the atom. Because of the importance of gaseous Na as a possible precursor to $Na_2SO_4(c)$ formation, data on these reactions should allow the evaluation of alternate mechanisms to those involving NaCl vaporization.

A kinetic and stoichiometric study of reaction (3) was carried out by using atomic absorption spectroscopy (to detect Na atoms) combined with microwave discharge-vacuum flow reactor techniques (to produce H atoms) over the temperature range 540 to 680K. The preliminary results (Ref. 4) indicated that H-atom attack of solid NaCl indeed produces Na-atoms even at these low temperatures. Because of the low temperature, NaCl vaporization is negligible and the corresponding homogeneous gas phase reaction

$$H(g) + NaCl(g) \rightarrow Na(g) + HCl(g) \quad (5)$$

plays no role in the Na(g) production observed in these studies. Combining the absorbances measured for Na(g) in the Arrhenuis rate expression with the Lambert-Beer Law, the apparent activation energy for reaction (3) of 5.2 kcal $mole^{-1}$ was obtained.

Reaction (4) was studied (Ref. 4) by using emission spectroscopy (to detect Na*(g)) combined with microwave discharge techniques (to generate O-atoms) in an O_2/Ar gas mixture. Even though the thermodynamics for this reaction would seem to be less favorable than those for reaction (3), Na*(g) was readily detectable between 510 and 620K. An Arrhenius treatment of the data for this reaction yielded an activation energy of 9.4 kcal $mole^{-1}$.

The fact that the reactions between solid NaCl and atomic hydrogen and oxygen exhibit such low activation energies is important in understanding the behavior of sodium in flame chemistry. High concentrations of H and O atoms exist in the reaction zone of hydrocarbon/air flames. The high diffusivity of the H atom makes reaction (3) seem to be particularly important as a mechanism for Na release and indicates that Na(g) may be released very early in the combustion process by a heterogeneous reaction. This process has thus freed Na atoms which can subsequently react to form other stable products without going through the route of sodium chloride vaporization. These considerations are especially relevant to aspects of the Na_2SO_4 deposition as will be discussed in the following section.

DEPOSITION PROCESS

The deposition of sodium sulfate from combustion gases containing sodium and sulfur is regarded as one of the fundamental steps in the phenomenon of hot corrosion of turbine components. Even though the primary concern of this paper is the chemistry of NaCl, it is through the formation and deposition of Na_2SO_4 that NaCl has its predominant, albeit indirect, effect in hot corrosion processes.

Recently, we described (Ref. 19) an equilibrium thermodynamic method of predicting condensation onset temperatures (dew points) of Na_2SO_4 in flame environments as a function of sulfur in the fuel and sea salt concentration in the intake air. The method consisted of applying the NASA complex chemical equilibrium computer program (Ref. 22). Thermodynamic properties of gaseous and condensed phase Na_2SO_4, along with additional species pertinent in sea salt-containing environments, were used in the program to calculate equilibrium combustion gas compositions and temperatures for representative turbine engine and burner rig flames. Compositions were calculated for various fuel/oxidant ratios with different concentrations of sulfur in the fuel and different concentrations of sea salt added to the intake air. Iterative calculations were made to determine the temperature below which condensation of Na_2SO_4 should be expected.

Deposition Experiments

To validate the thermochemical dew point predictions and to provide the basis for development of a deposition rate theory, experiments have been carried out by using a Mach 0.3 atmospheric pressure burner rig as shown schematically in Figure 6 (Ref. 6). A characteristic of the burner rig that was important in this study was the residence time of the dopant in the flame. Residence time is here defined as the time interval between introduction of the salt-containg aerosol into the burner and the arrival of the salt at the collector. Calculations based on the geometry of the rig and the gaseous flow velocity revealed that the residence time was 2.2 milliseconds. The burner used Jet A-1 fuel. The air was seeded with about 10 wppm of an inorganic sodium salt (NaCl, sea salt or Na_2SO_4). Deposits were collected on a cylindrical platinum target situated in the combustion gases. The deposition rate was determined at different collector target temperatures. It was anticipated that accuracy of theoretical predictions for a burner rig environment would lend credence to eventual predictions for actual turbine engine conditions, and to specifications for operating parameters necessary for more realistic burner rig simulation of engine conditions.

The results of the experiments that used sea salt and NaCl seeding are given in Figures 7 and 8. Chemical analysis, X-ray diffraction, and energy dispersive spectrometry analysis showed that the deposits consisted of mainly Na_2SO_4 with minor amounts of K_2SO_4, $CaSO_4$, and MgO from the sea salt runs; they consisted of pure Na_2SO_4 from the NaCl runs. A SEM micrograph of a deposit from a sea salt experiment, shown in Figure 9, disclosed that the deposit consisted of crystalline needles protruding from a fibrous mat. The appearance of the crystals indicates that the deposition occurred by vapor deposition of molecules, and not be impaction or capture of particles. Chemical analysis of the water solutions leached from the targets revealed that no soluble Cl^- was present in the deposits above background levels. Thus the chemical identification of the deposit composition was in agreement with the predictions of the chemical equilibrium computer program. The experimental condensation onset temperatures also agreed within the experimental uncertainties (±15K) with the predicted temperatures calculated from thermochemical data.

Our observation of the deposition of Na_2SO_4 from a burner rig combustor after a residence time of the order of only 2 milliseconds is taken by us to be of special significance. This observation and those made in the flame sampling studies are in apparent disagreement with the results reported by Hanby (Ref. 24). An accurate analysis of Hanby's results is complicated by the nature of his experimental arrangement. Because of the way his dilution air was added, one cannot define the exact fuel/air ratio in different sections of his combustor-tunnel. We would predict from equilibrium calculations for Hanby's case of 5% excess air that no Na_2SO_4 would be expected to form in his experiment. Apparently he detected Na_2SO_4 only after the fuel/air ratio of the combustion products was changed by the addition of dilution cooling air. This situation makes definition of residence time uncertain and indicates that the 8 milliseconds he reported for the formation of Na_2SO_4 might be in considerable error.

Deposition Theory

During the course of this research, it became obvious that a theoretical prediction was desirable for the rates of deposition of $Na_2SO_4(c)$ at surface temperatures below the deposition onset temperature. Toward this end, a comprehensive yet tractable mass transfer equation was developed for making such predictions by a NASA-sponsored collaborative effort between Professor D. E. Rosner and associates at Yale University and NASA personnel (Ref. 6-8). The experimental data obtained from the burner rig experiments provided a useful basis for developing and validating a deposition rate theory. It should be noted, however, that a gas turbine engine is a much more complicated system than the burner rig described here. The engine operates at significantly higher pressure and mass flow, and with complex mixing of fuel and air in the different sections. Thus, the applicability of the developed theory to engines remains to be demonstrated.

The experimental verification of a "dew point" surface temperature above which no deposition of $Na_2SO_4(c)$ was observed suggested to us that under the burner rig test conditions, deposition was associated with vapor diffusion to the collector across a "boundary layer". Furthermore, the nature of the crystalline needles in the collected deposit, as shown in Figure 9, suggests vapor deposition rather than particle capture or impaction. Accordingly, a convective diffusion theory employing multicomponent vapor transport for predicting Na_2SO_4 deposition rates in the burner rig experiments is being developed. However, the theory is also sufficiently general to be able to include transport by particles small enough to behave like heavy vapor molecules. In the theory development, two simplifying assumptions have been made: (1) all sodium added to the combustion gases is available for transport to the target via vapor species and (2) while local thermochemical equilibrium is achieved at the outer and inner edges of the concentration boundary layer around the collector, no homogeneous chemical reactions occur within the diffusion boundary layer. Thus the boundary layer is said to be chemically "frozen". This latter assumption markedly reduces computational time. The theory is referred to as the chemically frozen boundary layer (CFBL) theory.

In contrast to previous treatments of vapor deposition (Ref. 17-18 and 25-26), the CFBL theory makes provision for the effects of: (1) Na-element transport via species of differing mobility (i.e., NaCl(g), NaOH(g), Na(g), Na_2SO_4(g)); (2) thermal (Soret) diffusion of heavy, Na-containing species; and (3) free stream turbulence intensity and scale. The formulation of the CFBL theory is presented in References 6 and 7.

The results of the application of the CFBL theory to the prediction of deposition rates for the sea salt and NaCl-seeded burner rig experiments are given in Figures 7 and 8. Agreement between maximum deposition rates far below the dew point (ca. 5 mg/hr.) predicted by the theory and those obtained in the experiments is good, but the predicted dependence on surface temperature exhibits plateau-like behavior not evident from the experiments. Nonetheless, the agreement is particularly encouraging in view of the fact that the burner rig was being seeded heavily with Na-compounds at the gram per hour level. The theory has also been used to predict the form of the dependence of the deposition rate on fuel sulfur content and on pressure level (Ref. 7-8).

While condensed phase Na_2SO_4 can be formally regarded as one of the diffusing species, in practice, our knowledge of the particle size distribution (hence Brownian and thermophoretic diffusion parameters) is presently inadequate to assess this contribution to the observed deposition rates. For this reason, and because of the highly undersaturated state of our seeded combustion products upstream of the target, only vapor diffusion has been included in our treatment up to the present time.

By examining the nature of the equilibrium calculated species concentrations in the combustion gas free stream and at the surface of the collector, some insight may be gained regarding the nature of the transporting species in the context of the CFBL theory. According to this model, Na_2SO_4(c) growth on a surface occurs primarily via transport of NaOH(g), NaCl(g), and Na(g), not Na_2SO_4(g). In fact the Na_2SO_4(g) species contributes to a net loss (not gain) of the condensate layer due to a negative concentration gradient for this species across the boundary layer. Thus in the CFBL framework, gas phase conversion of NaCl to Na_2SO_4 in the available residence time is not necessary for the process of Na_2SO_4 deposition. Rather, of more importance are heterogeneous reactions at the gas/liquid interface which convert NaCl(g), NaOH(g), and Na(g) to Na_2SO_4(l) in the presence of excess O_2 and S-containing vapor species. Of course, the mechanism of this conversion may involve a Na_2SO_4 molecule. This situation makes it clear that a multicomponent deposition theory is absolutely essential in engineering applications.

An interesting aspect of calculations of combustion gas and deposit compositions was consideration of what condensed phases, other than Na_2SO_4 might be expected to deposit from sodium-seeded combustion gases. Na_2SO_4 was the only condensate expected over a wide range of temperatures with an equivalence ratio of less than one (i.e. oxidizing conditions). Under the conditions investigated, the calculations predict that no NaCl or NaOH condensates form. Even if Na_2SO_4(c) were prohibited from forming (by omitting data for this phase from the program library) no NaCl or NaOH condensates

would form. Our calculations show that the phase that would likely form from a thermodynamic viewpoint would be Na_2CO_3, which is much more stable in a combustion gas environment than NaCl(c). The high stability of the chlorine-containing HCl molecule is also important here. This phenomenon is an illustration that even though a molecule with a certain stoichiometry (such as NaCl) is one of the more stable gases in a complex equilibrium, the same composition may not be the most stable condensed phase. Indeed, the deposition of Na_2CO_3 has been observed from Na-seeded sulfur-free propane/air flames (Ref. 27). Thus it is not surprising that in practice NaCl is rarely detected as a condensed phase deposit in turbine engines or burner rigs. Situations in which NaCl deposits were observed (Refs. 28,29,30,31, and 32), at levels greater than those predicted by Raoult's Law (Ref. 33), must be attributed to particle capture and the existence of a metastable condition.

Condensed Phase NaCl to Na_2SO_4 Conversion

In practice NaCl is rarely detected, or is only detected at extremely low levels, on components from turbine engine hot-gas-path sections. However, "compressor NaCl shedding theories" (Ref. 15, 16) and similar ideas suggest that it should be possible for NaCl to deposit by particle impaction. The question then arises whether the reaction of impacted NaCl(c) with SO_2 and O_2 to form Na_2SO_4(c) and a gaseous Cl-containing species is the reason why chloride is not detected in deposits. The fundamental chemistry of this conversion reaction is currently being investigated by W. L. Fielder and the authors at Lewis Research Center. A knowledge of the kinetics for this conversion process should be useful in interpreting the behavior of NaCl particles which deposit by impaction.

The reaction of single crystals of NaCl at 600 to 900K with flowing mixtures of O_2 and SO_2 is being studied at atmospheric pressure by thermogravimetric and mass spectrometric techniques. Parameters included in the investigation include temperature, gas flow rate, and SO_2-SO_3 concentration.

Preliminary results over the temperature range of 600 to 900K for the reaction with an initial concentration of 8 mole % SO_2 in O_2 are shown by an Arrhenius-type plot in Figure 10. The data points shown were obtained from a number of individual NaCl single crystals and have been combined into one plot. The activation energy calculated from the data in Figure 10 is 12 kcal $mole^{-1}$. This low value indicates that the NaCl to Na_2SO_4 conversion can take place readily even at moderate temperatures, and this may explain the observation that Cl^- is rarely detected in deposits from combustion systems. Thermodynamics predicts that essentially no condensed phase NaCl should exist. Of course, a small amount of NaCl should dissolve in Na_2SO_4 according to Raoult's Law for solutions (Ref.33). The low activation energy observed for the reaction indicates that only small kinetic barriers exist to prevent the chemical equilibrium from being achieved.

Interaction of NaCl(g) and HCl(g) with Na_2SO_4

Several investigators have reported that NaCl(g) apparently acted to induce dissociation or vaporization of Na_2SO_4(c) (e.g., Ref. 34-36). Thus the interaction of Na_2SO_4(l) with NaCl(g), HCl(g), and H_2O(g) was studied

in atmospheric pressure flowing air and oxygen at $Na_2SO_4(l)$ temperatures of 900 and 1000K (Ref. 33). Thermogravimetric and high pressure mass spectrometric sampling techniques were used in the investigation. The experimental results established that previously reported enhanced rates of weight loss of $Na_2SO_4(l)$ in the presence of NaCl(g) are due to the reaction

$$2\ NaCl(g) + SO_2(g) + H_2O(g) + 1/2\ O_2(g) = Na_2SO_4(l) + 2\ HCl(g) \quad (6)$$

being driven to the left in flowing gas systems. The loss of SO_2 from the system results in a net loss of Na_2SO_4 and because SO_2 is not being replaced as a reactant, the amount of $Na_2SO_4(l)$ in the system decreases. The HCl(g) needed to drive the reaction to the right is formed by the hydrolysis of NaCl caused by small but significant amounts of $H_2O(g)$ present in most experimental systems (and always present in combustion gases) by the reaction

$$NaCl(g) + H_2O(g) = NaOH(g) + HCl(g) \quad (7)$$

Supplementing the experimental observations are thermochemical calculations which show that even with sub-ppm levels of $H_2O(g)$ present, significant quantities of HCl(g) should be produced.

REACTIONS WITH OXIDES

Equilibrium thermodynamic calculations indicate that the engine hot section, under conditions conducive to hot corrosion, should be relatively rich in the contaminant gases NaCl, NaOH, and HCl (Ref. 19). These chemical species are generally considered as highly reactive at high temperatures, and therefore it seems reasonable to expect that they might play a significant role in the hot corrosion process. Previously it had been demonstrated that adverse effects could be associated with exposure of hot oxidizing metals to partial pressures of NaCl(g) (e.g., see Refs. 36 - 40). The major effects observed were: (1) NaCl(g) could compromise the so-called protective oxide scale on certain superalloys by degrading the oxide adherence which resulted in spalling; (2) NaCl(g) removed chromium from samples as a volatile chromium compound; and (3) NaCl(g) could accelerate the degradation, by sulfidative oxidation, of certain CoCrAlY-coated alloys (Ref. 36).

In addition to gas phase NaCl, solid or liquid NaCl may come into contact with oxide surfaces in turbines. It has been shown (Ref. 16) that compressors of gas turbine engines can physically collect some solid sodium chloride and sulfate from the sea salt aerosol. These deposits can be periodically shed from the compressor and pass to the hot section of the turbine. The particles may then vaporize, react, impact on turbine surfaces, or pass through the engine. It has been well established that condensed NaCl or $NaCl-Na_2SO_4$ mixtures can be very corrosive (e.g., see Refs. 41 - 45). However, to date, such studies have not been a part of the NASA program which has concentrated on the role of gaseous NaCl in relation to corrosion-related processes.

Volatile Products Studies

Cooled target vapor collection techniques were used to study the formation of volatile products when samples of Cr, Mo, and several superalloys were exposed at elevated temperatures to oxidizing environments containing NaCl(g) and H_2O(g) (Refs. 9 and 10). High pressure mass spectrometric sampling was used to identify directly the volatile product molecules emanating from these materials. Schematics of the respective apparatus are shown in Figure 11. The metal samples were suspended in a furnace and mixtures of O_2 and NaCl(g) with and without added H_2O(g) were slowly passed over the samples. In the target collection experiments, volatile products were condensed on water-cooled platinum targets, subsequently dissolved in water, and the resulting solutions analyzed for metal cations by atomic absorption and/or emission spectroscopy. The identification of the volatile species was accomplished with the high pressure mass spectrometric sampler.

The target collection experiments with chromium showed that the rate of transport of chromium as a volatile species was significantly enhanced when H_2O(g) and/or NaCl(g) was added to the oxidizing environment. The experiments are discussed in References 9 and 10. For chromium and chromia-forming alloys, the volatile species were identified by mass spectrometry as being primarily $(NaCl)_xCrO_3$ where x = 1, 2, or 3 and $(NaOH)_yCrO_3$ where y = 1 or 2. The mass spectral data that lead to these identifications for this system are shown in Figure 12. Similar results were obtained at lower temperatures ($\sim$675°C) for molybdenum where the major species identified were $(NaCl)_x(MoO_3)_3$ and $NaOH(MoO_3)_3$. We believe that the complex vapor species observed in our studies were the first examples of such gaseous alkali halide-metal oxide complexes. In this regard, one point must be emphasized: the fact that the rate of transport of chromium was found to increase in the target experiments when NaCl(g) was added to the system Cr_2O_3(g) + O_2(g) indicates that the rate is not limited by the vaporization rate of CrO_3(g). The only volatile species formed in the absence of NaCl(g) was CrO_3(g). Therefore, the Na/Cr-containing species are not products of homogeneous gas phase reactions but are formed by heterogeneous reactions. Furthermore, because species such as $(NaCl)_xCrO_3$ are not the product of gas phase reactions, they likewise cannot be the product of sampling artifacts such as clustering or beam condensation in the high pressure sampler.

An exhaustive search was made for the frequently proposed vapor molecules CrO_2Cl_2, $CrCl_2$, $CrCl_3$, and Na_2CrO_4. This effort was unrewarding and only a trace of the species $Na_2Cr_2O_7$(g) was detected in addition to the previously identified chemical complexes. However, this is not to say that some of the aforementioned species will not form under other conditions, e.g., at low oxygen pressure, in a vacuum, or in the absence of sodium. Certainly it is expected that Na_2CrO_4(g), which has been identified as a stable molecule in vacuum by a Knudsen cell-mass spectrometry study (Ref. 46), would form when Na_2SO_4 reacts with Cr_2O_3 in O_2 in the absence of any chlorine.

We have concluded that the main reactions responsible for the vapor transport of chromium in various situations are:

$$1/2\ Cr_2O_3(c) + 3/4\ O_2(g) = CrO_3(g) \quad (8)$$

$$1/2\ Cr_2O_3(c) + 3/4\ O_2(g) + H_2O(g) = CrO_2(OH)_2(g) \quad (9)$$

$$1/2\ Cr_2O_3(c) + 3/4\ O_2(g) + xNaCl(g) = (NaCl)_xCrO_3(g),\ x = 1,\ 2,\ or\ 3 \quad (10)$$

$$1/2\ Cr_2O_3(c) + 3/4\ O_2(g) + xNaOH(g) = (NaOH)_xCrO_3(g),\ x = 1\ or\ 2 \quad (11)$$

Various measured kinetic parameters for Reactions (8) and (10) are reported in Reference 9. For molybdenum, the main reaction responsible for the vapor phase transport were deduced to be:

$$xMoO_3(c) = (MoO_3)_x(g),\ x = 3\ or\ 4 \quad (12)$$

$$MoO_3(c) + H_2O(g) = MoO_2(OH)_2(g) \quad (13)$$

$$3\ MoO_3(c) + xNaCl(g) = (NaCl)_x(MoO_3)_3(g),\ x = 1\ or\ 2 \quad (14)$$

$$3\ MoO_3(c) + NaOH(g) = NaO_4(MoO_3)_3(g) \quad (15)$$

The molecules that were identified are felt to be the ones responsible for the vapor phase transport of the respective metals in corrosive salt-containing atmospheres. They appear to be more thermodynamically stable under oxidizing conditions in the presence of NaCl(g) than the other previously postulated species.

It is intriguing to postulate what the role of the complex vapor molecules might be in the corrosion process. Thinning of a chromium oxide scale could result in the formation of regions of aggravated stress where cracking might occur, thus compromising the scale. Also, a thinned section of scale might be more readily breached or fluxed by $Na_2SO_4(l)$. In either case, NaCl(g) attack compromises the oxide scale and thus promotes hot corrosion attack. It is important to emphasize that although the degree of attack by NaCl(g) is of a much smaller magnitude than the $Na_2SO_4(c)$ hot corrosion attack, the NaCl(g) attack may be of comparable importance in the overall high temperature corrosion processes.

Effect of NaCl(g) on Oxidation and Hot Corrosion of NiAl and NiCr

To complement the volatile species studies described directly above, J. G. Smeggil and N. S. Bornstein of United Technologies Research Laboratories have investigated, under NASA Contract No. NAS3-20039, the effect of NaCl(g) on the oxidation and Na_2SO_4-induced hot corrosion of NiAl and several chromia-forming alloys. The results of these studies are given in References 11 to 14.

In brief, the thermogravimetric oxidation studies and metallography have demonstrated an effect of NaCl(g) on the oxidation of

NiAl (Refs. 11 and 13). Even at low concentrations, (ppm levels) NaCl vapor substantially modifies the high temperature oxidation behavior of the alumina-former NiAl. The role of the NaCl(g) is two-fold. Firstly, aluminum is removed from a dense protective Al_2O_3 scale and redeposited on the surface of the scale as Al_2O_3 whiskers. This effect is illustrated in Figure 13. Secondly, the NaCl vapor effects isothermal spallation of the normally protective Al_2O_3. The interaction of NaCl(g) with NiAl is not expected to be unique and likely occurs with other alumina-forming surface coatings and substrate compositions. At this time, the mechanism of whisker growth and spalling is not completely understood, although vapor phase and grain boundary diffusion might account for the observations.

In the incubation period associated with Na_2SO_4-induced hot corrosion of NiAl, NaCl(g) has been shown to be effective in removing aluminum from below the protective alumina scale and redpositing it as Al_2O_3 whiskers on the surface of the Na_2SO_4-coated sample (Refs. 11 and 14). The removal of aluminum from below the surface of the oxide layer locally depletes the substrate of aluminum and leads to a progressive weakening of the protective scale-substrate bond. Upon rupture of the protective Al_2O_3 scale, the substrate locally has an insufficient aluminum activity to reform the protective layer. At low temperatures, the diffusion rates are not high enough to allow aluminum to reform the protective Al_2O_3 scale. This condition has been shown in oxidation studies to be sufficient to cause accelerated oxidation rates.

The oxidation behavior of elemental chromium and Ni-25Cr have been studied at 900 and 1050°C in oxygen atmospheres with and without the addition of gaseous NaCl (Refs. 11 and 12). Effects arising from the presence of small concentrations of NaCl(g) are reflected both in thermogravimetric data as illustrated in Figure 14 and in the microstructure of the oxide scales formed. For Ni-25Cr, "S"-shaped oxidation curves are obtained when NaCl(g) is present in the oxidizing environment. This curve shape suggests breakaway oxidation kinetics for Ni-25Cr with NaCl(g) while no such breakway is seen for pure chromium. The removal of chromium from chromia scales on Ni-25Cr affects the formation of a zone depleted of chromium in the alloy substrate adjacent to the scale. With the consequently reduced activity of chromium thermodynamic considerations favor the formation of the spinel $NiCr_2O_4$. Thus the breaks observed in the thermogravimetric data are taken to represent and correspond to the conversion of the scale from the protective chromia to the somewhat less protective spinel.

In simple oxidation the effect of NaCl(g) on B-1900 was found to be similar to that observed for NiAl, i.e., α-Al_2O_3 crystals were deposited on the surface of the normally dense protective oxide. Regions extensively depleted of gamma prime precipitates were frequently observed in the underlying substrate. Except for the obvious absence of sulfide precipitates, the observed substrate microstructures were analogous to those found in the Na_2SO_4-induced laboratory hot corrosion of this alloy.

CONCLUDING REMARKS

The chemical studies reviewed here have helped elucidate the possible roles that NaCl can play in the overall hot corrosion process. Besides being a source of sodium for the formation of corrosive liquid Na_2SO_4, the NaCl itself contributes in other indirect ways to the material degradation associated with the high temperature environmental attack. Additionally, the experimental results lend credence to the conceptual scheme presented in Figure 1 and resolve conflicting aspects of the NaCl misconceptions noted at the outset in the Introduction.

Certainly the chemistry and kinetics related to NaCl in combustion environments will have analogs in other alkali salt systems which might be more pertinent to alternate fuels for use in directly fired heat engines. Likewise, the methodology developed in the NaCl studies reviewed here can be applied to other situations where impure fuels and/or industrial environments are being considered. At the Lewis Research Center some of the methodology is being applied in the Critical Research and Advanced Technology Project (CRT) sponsored by the Department of Energy (DOE) (ERDA/NASA interagency agreement EF-77-A-01-2549). We are using equilibrium calculations and burner rig tests to ascertain the composition and amounts of deposits to be expected with various fuels containing numerous impurities. These calculations have value in predicting the behavior of complex systems and they represent a first step in understanding the chemistry involved in flames and combustion products.

As part of the CRT program, calculations are being made for solvent refined coal (SRC-II) fuels taking into account the trace metal content of the fuels (REF. 47). At present we are considering more than 20 elements and more than 450 phases in our calculations. Some of the major phases are listed in Table I. In the NaCl-S work seventy condensed and gas phase species (for the elements C, H, O, S, Na, and Cl) were considered to arrive at the molecular species combustion product distributions given in Figure 4. Obviously the coal-related case in considerably more complex than the work where NaCl and sulfur were the only impurities. For SRC-II, predicted deposition composition and dew points are being compared with experimental results obtained in burner rig tests.

REFERENCES

1. C. A. Stearns, R. A. Miller, F. J. Kohl, and G. C. Fryburg, NASA TM X-73600 (1977).

2. G. C. Fryburg, R. A. Miller, C. A. Stearns, and F. J. Kohl, in "High Temperature Metal Halide Chemistry," D. L. Hildenbrand and D. D. Cubicciotti, Eds., p. 468, The Electrochemical Society Softbound Symp. Series, Vol. 78-1, Princeton, NJ, 1978; also NASA TM-73794 (1977).

3. C. A. Stearns, R. A. Miller, F. J. Kohl, and G. C. Fryburg, J. Electrochem. Soc. 124, 1145 (1977).

4. D. E. Rosner, First Semiannual Report on NASA Grant No. NSG-3169, Yale University, May 1978, NASA CR-159612.

5. D. E. Rosner, Second Semiannual Report on NASA Grant No. NSG-3169, Yale University, Nov. 1978, NASA CR-159613.

6. F. J. Kohl, G. J. Santoro, C. A. Stearns, G. C. Fryburg, and D. E. Rosner, J. Electrochem. Soc. 126, 1054 (1979); also NASA TM X-73683 (1977).

7. D. E. Rosner, B. -K. Chen, G. C. Fryburg, and F. J. Kohl, Combustion Science and Technology, in press.

8. D. E. Rosner, K. Seshadri, J. Fernandez de la Mora, G. C. Fryburg, F. J. Kohl, C. A. Stearns, and G. J. Santoro, in "Proceedings of the Tenth Materials Research Symposium: Characterization of High Temperature Vapors and Gases," National Bureau of Standards, Washington, DC, Sept. 1978, in press.

9. C. A. Stearns, F. J. Kohl, and G. C. Fryburg, in "Properties of High Temperature Alloys," Z. A. Foroulis and F. S. Pettit, Eds., p. 655, The Electrochemical Society Softbound Symposium Series, Vol. 77-1 Princeton, NJ, 1977; also NASA TM X-73476 (1976).

10. G. C. Fryburg, R. A. Miller, F. J. Kohl, and C. A. Stearns, J. Electrochem. Soc. 124, 1738 (1977); also NASA TM X-73599 (1977).

11. J. G. Smeggil and N. S. Bornstein, NASA CR-135348 (1977).

12. J. G. Smeggil and N. S. Bornstein, in "High Temperature Metal Halide Chemistry," D. L. Hildenbrand and D. D. Cubicciotti, Eds., p. 521, The Electrochemical Society Softbound Symposium Series, Vol. 78-1, Princeton, NJ, 1978.

13. J. G. Smeggil and N. S. Bornstein, J. Electrochem. Soc. 125, 1283 (1978).

14. J. G. Smeggil, N. S. Bornstein, and M. A. DeCrescente, in "Ash Deposits and Corrosion Due to Impurities in Combustion Gases," R. W. Bryers, Ed., p. 271, Hemisphere Publishing Corp., Washington, DC, 1978.

15. I. I. Bessen and R. E. Fryxell, in "Gas Turbine Materials Conference Proceedings," p. 73, Naval Ship Engineering Center, Naval Air Systems Command, Washington, DC, 1972.

16. R. E. Fryxell and I. I. Bessen, in "Proceedings of the 1974 Gas Turbine Materials in the Marine Environment Conference," p.259, J. W. Fairbanks and I. Macklin, Eds., MCIC-75-26, 1974.

17. C. G. McCreath, in "Third Conference on Gas Turbine Materials in a Marine Environment," Session V, Paper 2, University of Bath, England, Sept. 1976.

18. A. B. Hedley, T. D. Brown, and A. Shuttleworth, J. Eng. Power 88, 173 (1966).

19. F. J. Kohl, C. A. Stearns, and G. C. Fryburg, in "Metal-Slag-Gas Reactions and Processes," Z. A. Foroulis and W. W. Smeltzer, Eds., p. 649, The Electrochemical Society Softbound Symposium Series, Princeton, NJ, 1975; also NASA TM X-71641 (1975).

20. JANAF Thermochemical Tables, Dow Chemical Co., Midland, MI, dated June 30, 1978 for $Na_2SO_4(g)$.

21. C. A. Stearns, F. J. Kohl, G. C. Fryburg, and R. A. Miller, in "Proceedings of the Tenth Materials Research Symposium: Characterization of High Temperature Vapors and Gases," National Bureau of Standards, Washington, DC, Sept. 1978, in press; also NASA TM-73720 (1977).

22. S. Gordon and B. J. McBride, NASA SP-273 (1971).

23. J. W. Hastie, "High Temperature Vapors," p. 217, Academic Press, NY, 1975.

24. V. I. Hanby, J. Eng. Power 96, 129 (1974).

25. T. D. Brown, J. Inst. Fuel 39, 378 (1966).

26. K. Ross, J. Inst. Fuel 38, 273 (1965).

27. R. A. Durie, J. W. Milne, and M. Y. Smith, Combustion and Flame 30, 221 (1977).

28. P. J. Jackson and H. C. Duffin, in "The Mechanism of Corrosion by Fuel Impurities," H. R. Johnson and D. J. Littler, Eds., p. 427, Butterworths, 1963.

29. J. Dunderdale and R. A. Durie, J. Inst. Fuel 37, 493 (1964).

30. W. D. Halstead and E. Raask, J. Inst. Fuel 42, 344 (1969).

31. R. J. Bishop and K. K. Cliffe, J. Inst. Fuel 42, 283 (1969).

32. C. G. Root and A. R. Stetson, Session V, Paper 7. "Third Conference on Gas Turbine Materials in a Marine Environment," University of Bath, England, Sept. 1976.

33. C. A. Stearns, F. J. Kohl, G. C. Fryburg, and R. A. Miller, in "High Temperature Metal Halide Chemistry," D. L. Hildenbrand and D. D. Cubicciotti, Eds., p. 555, the Electrochemical Society Softbound Symposium Series, Vol. 78-1, Princeton NJ, 1978; also NASA TM-73796 (1977).

34. E. J. Felten and F. S. Pettit, Pratt and Whitney Quarterly Report, March 1, 1976 - May 31, 1976, NRL Contract No. N00173-76-C-0146.

35. T. J. Radzavich and F. S. Pettit, Pratt and Whitney Quarterly Report, June 1, 1976 - August 31, 1976, NRL Contract No. N00173-76-C-0146.

36. R. L. Jones and S. T. Gadomski, J. Electrochem. Soc. 124, 1641 (1977).

37. J. F. C. Condé and B. A. Wareham, in Ref. 16 p. 73.

38. P. Hancock, in Ref. 16, p. 225.

39. J. B. Johnson, J. R. Nicholls, R. C. Hurst, and P. Hancock, Corr. Sci. 18, 527 (1978).

40. M. K. Horsain and S. R. J. Saunders, Oxid. Metals 12, 1 (1978).

41. P. M. Johnson, D. P. Whittle, and J. Stringer, Corr. Sci. 15, 721 (1975).

42. D. W. McKee, D. A. Shores, and K. L. Luthra, J. Electrochem. Soc. 125, 411 (1978).

43. C. A. C. Sequeira and M. H. Hocking, J. Appl. Electrochem. 8, 179 (1978).

44. F. Mansfeld, N. E. Paton, and W. M. Robertson, Met. Trans. 4, 321 (1973).

45. R. H. Barkalow and F. S. Pettit, "Degradation of Coating Alloys in Simulated Marine Environments," NRL Contract No. N-00173-76-C-0146, Final Report, June 15, 1978.

46. C. A. Stearns, F. J. Kohl, R. A. Miller, and G. C. Fryburg, NASA TM-79210 (1979).

47. R. B. Callen, J. G. Bendoraitis, C. A. Simpson and S. E. Voltz, Ind. Eng. Chem. Prod. Res. Dev. 15, 222 (1976).

TABLE I. - METAL-CONTAINING COMPOUNDS AND MAJOR COMMON GASEOUS COMBUSTION PRODUCTS CONSIDERED IN THERMODYNAMIC EQUILIBRIUM CALCULATIONS FOR IMPURE FUELS DEPOSITION STUDIES

Element	Compounds and phases*
Na	$NaCl(g,c)$, $NaOH(g)$, $Na_2SO_4(g,c)$, $Na_2CO_3(c)$, $Na_2V_2O_6(c)$, $Na_2Fe_2O_4(c)$ $Na_2SiO_3(c)$, $NaAlO_2(c)$, $Na_2TiO_3(c)$
K	$KCl(g,c)$, $KOH(g)$, $K_2SO_4(g,c)$, $K_2S(c)$, $K_2CO_3(c)$
Ni	$NiO(g,c)$, $Ni(OH)_2(g)$
Cr	$CrO_2(g)$, $CrO_3(g)$, $Cr_2O_3(c)$, $NiCr_2O_4(c)$
Cu	$CuO(g,c)$ $CuCl(g)$, $Cu_2O(c)$
Fe	$FeO(g)$, $Fe(OH)_2(g)$, $Fe_2O_3(c)$, $NiFe_2O_4(c)$, $CuFe_2O_4(c)$
Mg	$Mg(OH)_2(g)$, $MgCl_2(g)$, $MgO(g,c)$, $MgSO_4(c)$, $MgAl_2O_4(c)$, $Mg_2TiO_4(c)$
Ca	$Ca(OH)_2(g)$, $CaCl_2(g)$, $CaO(g,c)$, $CaSO_4(c)$
Ba	$Ba(OH)_2(g)$, $BaCl_2(g)$, $BaO(g,c)$, $BaSO_4(c)$
Al	$AlO_2(g)$, $Al_2O(g)$, $AlOCl(g)$, $Al_2O_3(c)$
Si	$SiO(g)$, $SiO_2(g,c)$
Ti	$TiO(g)$, $TiO_2(g,c)$, $TiOCl_2(g)$
V	$VO(g)$, $VO_2(g)$, $V_2O_5(c)$
Zn	$ZnO(g,c)$, $ZnSO_4(c)$
Pb	$PbO(g,c)$, $PbCl(g)$, $PbSO_4(c)$
H	$H_2(g)$, $H_2O(g)$, $HCl(g)$
O	$O_2(g)$, $OH(g)$
N	$N_2(g)$, $NO(g)$, $NO_2(g)$, $N_2O(g)$
C	$CO(g)$, $CO_2(g)$
S	$SO_2(g)$, $SO_3(g)$, $H_2S(g)$, $H_2SO_4(g)$

*For phases g represents gas and c represents condensed.

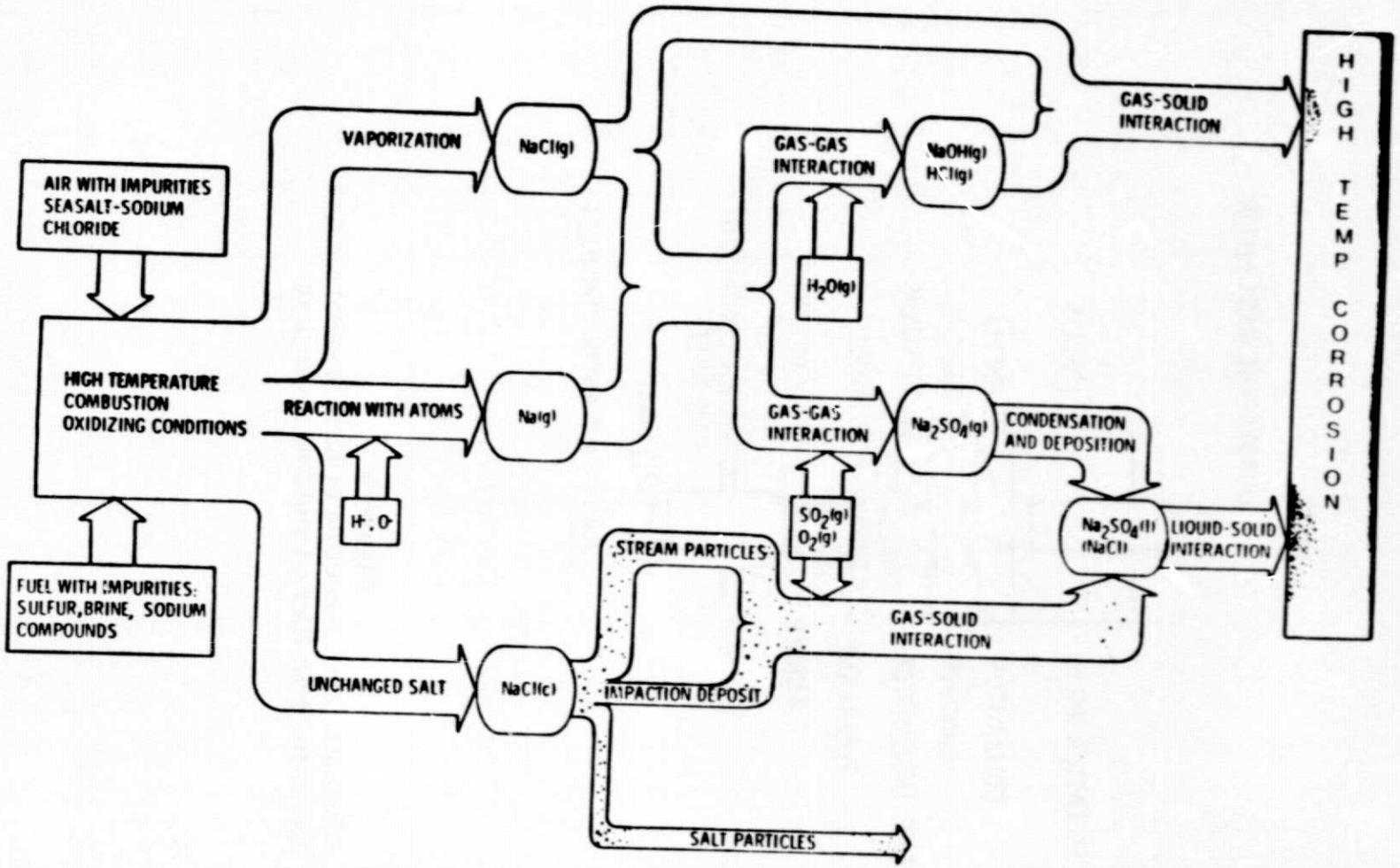

Figure 1
Behavior of NaCl in a turbine engine combustion gas environment.

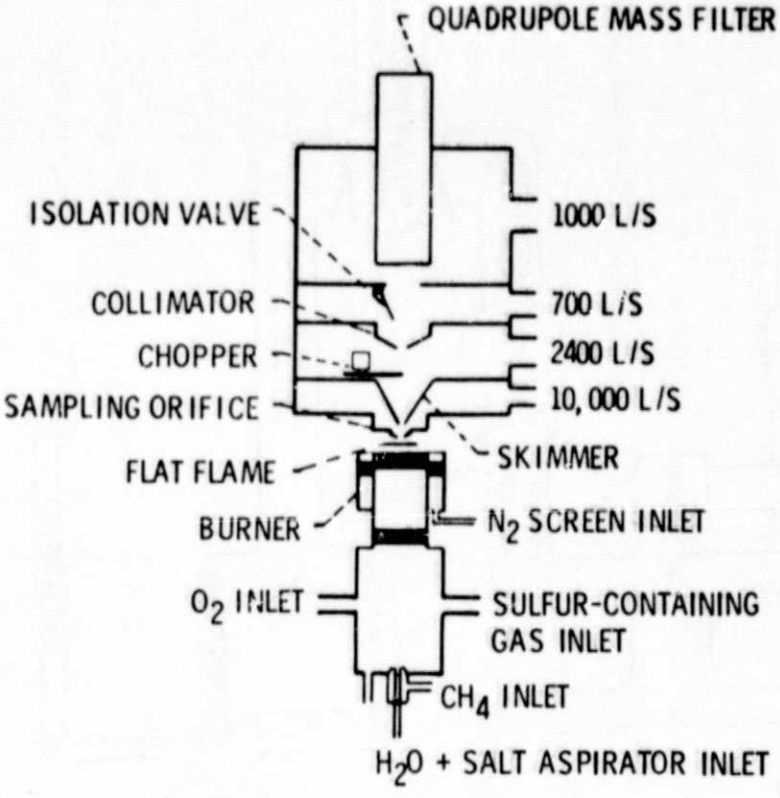

Figure 2
Schematic cross-section of high pressure mass spectrometric flame sampling apparatus.

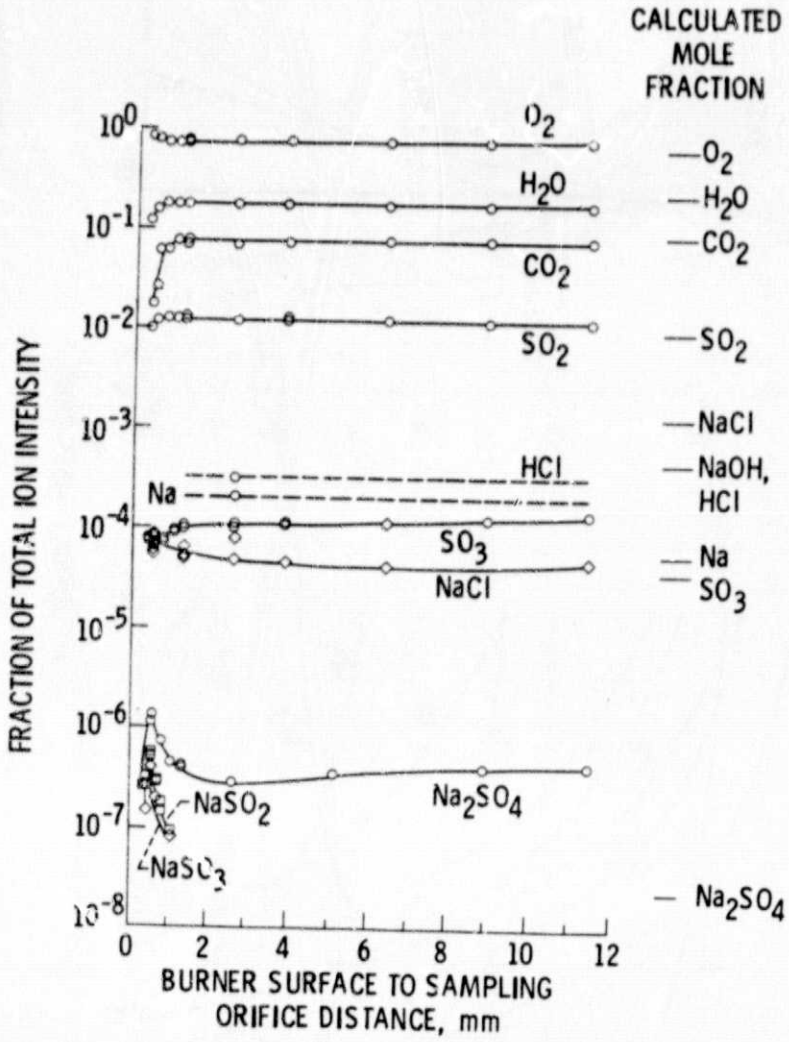

Figure 3

Composition profiles for a methane-oxygen flame doped with NaCl and SO_2. Fuel to oxidant mass ratio was 0.072 and mole percent of reactants was: 8.9 CH_4, 84.1 O_2, 5.9 H_2O, 0.18 NaCl and 0.92 SO_2. Calculated mole fractions refer to the adiabatic flame temperature of 2032K.

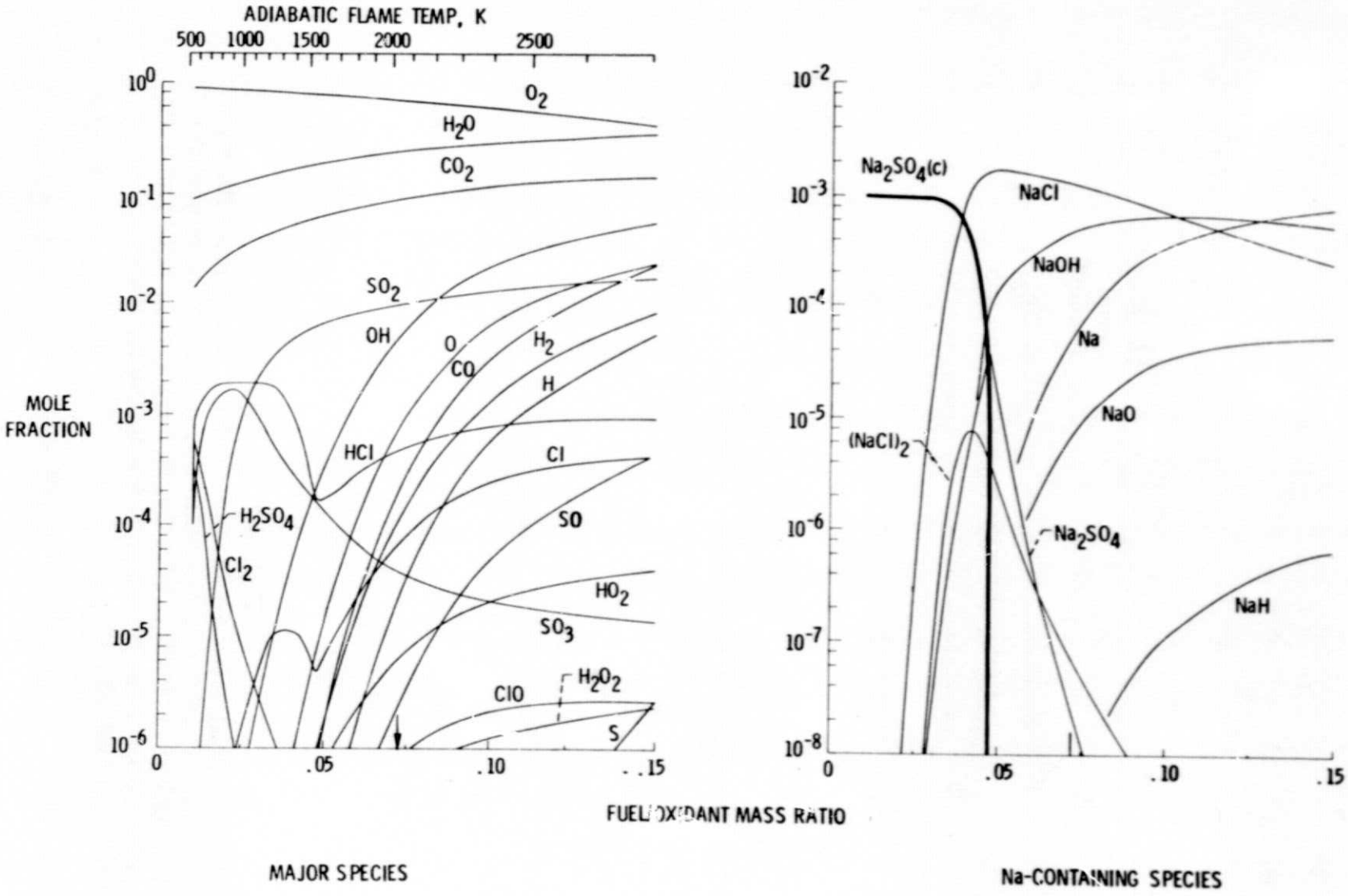

Figure 4

Equilibrium chemical composition for $NaCl$-SO_2 doped methane-oxygen flame with fuel to oxidant mass ratio of 0.072 and mole percent of reactants fixed at 8.9 CH_4, 84.1 O_2, 5.9 H_2O, 0.18 NaCl and 0.92 SO_2.

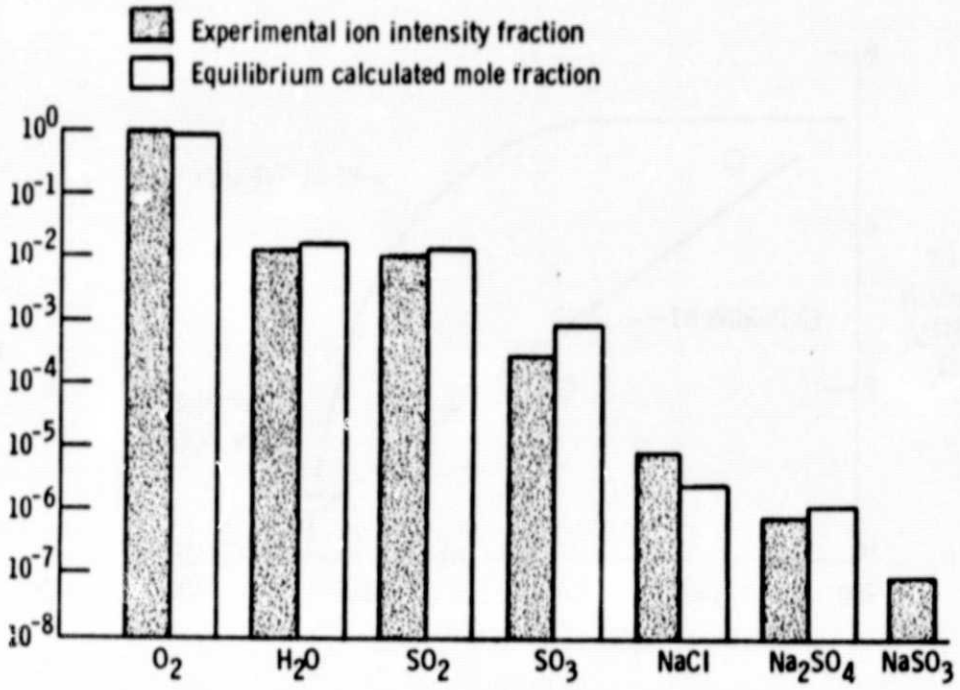

Figure 5
Comparison of measured and equilibrium calculated reaction products for the flowing gas mixture of NaCl + SO_2 + H_2O + O_2 at a temperature of 1413K.

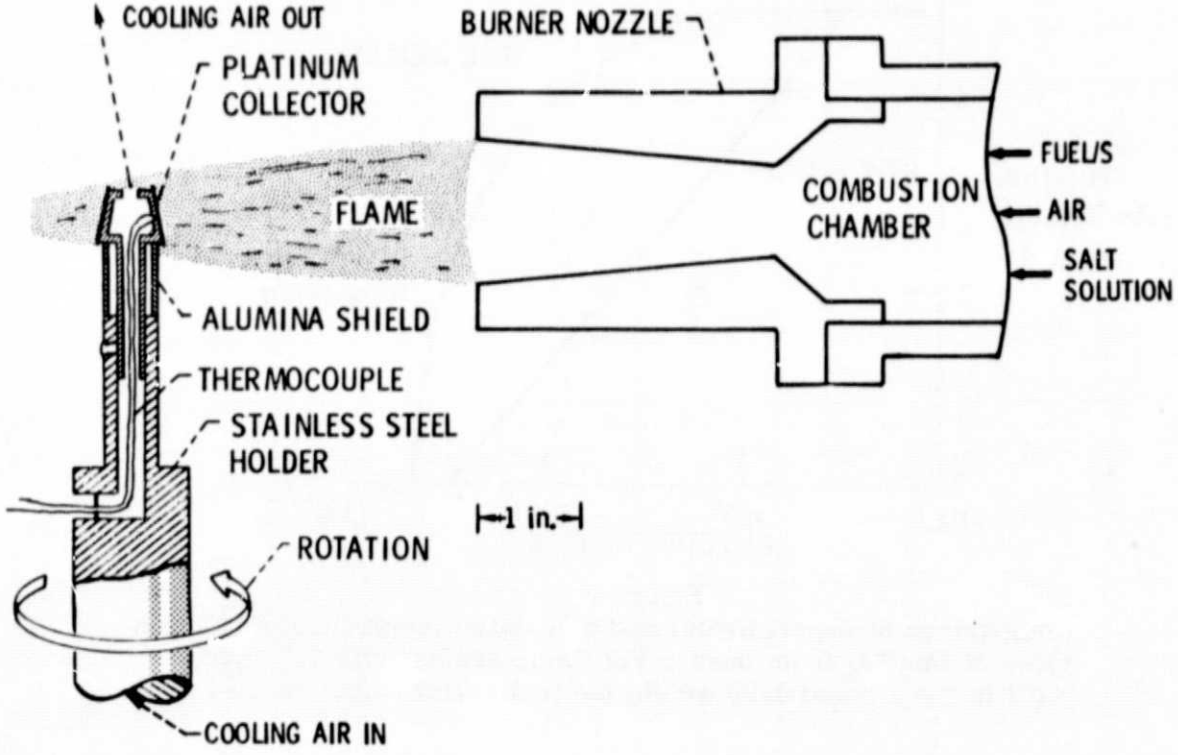

Figure 6
Schematic cross-section of burner rig deposition apparatus.

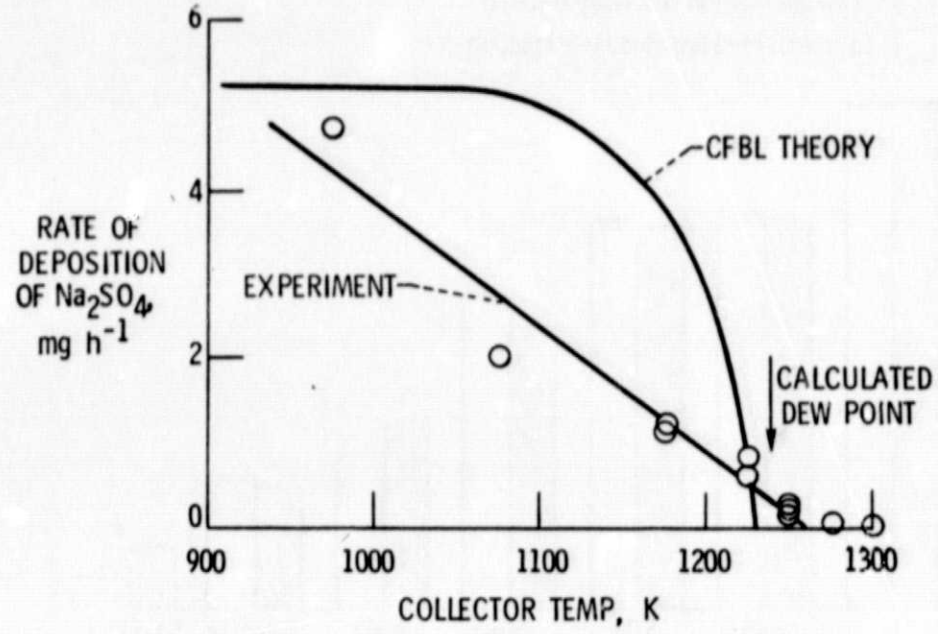

Figure 7

Comparison of experimental and calculated theoretical deposition rates of Na_2SO_4 from burner rig seeded with 11.3 wppm sea salt and 0.038 weight percent sulfur in the Jet A-1 fuel.

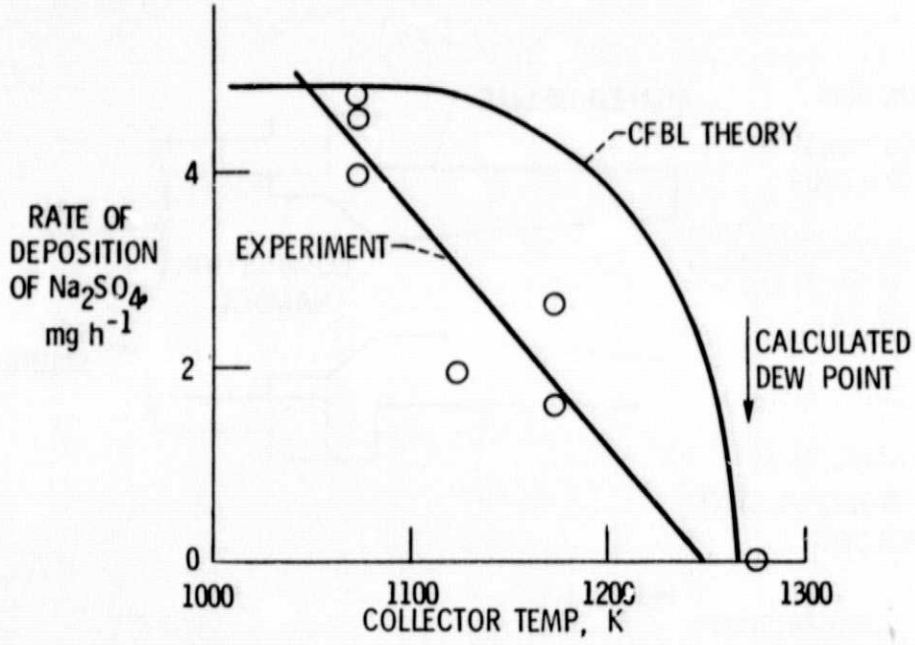

Figure 8

Comparison of experimental and calculated theoretical deposition rates of Na_2SO_4 from burner rig flame seeded with 8.0 wppm of NaCl in the air and 0.25 weight percent sulfur in the Jet A-1 fuel.

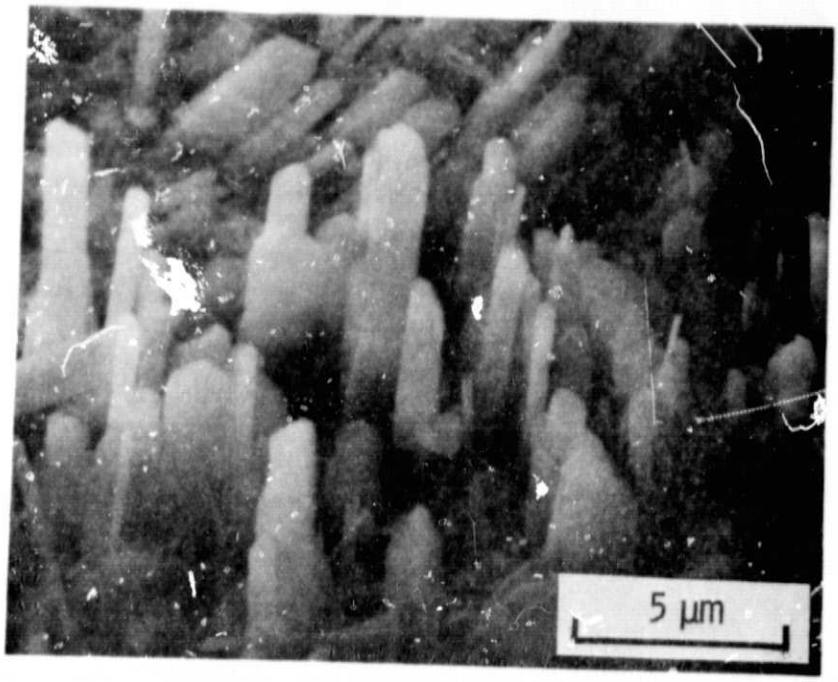

Figure 9
SEM micrograph of deposit collected from burner rig flame combustion gases seeded with 11.3 wppm ses salt in the air.

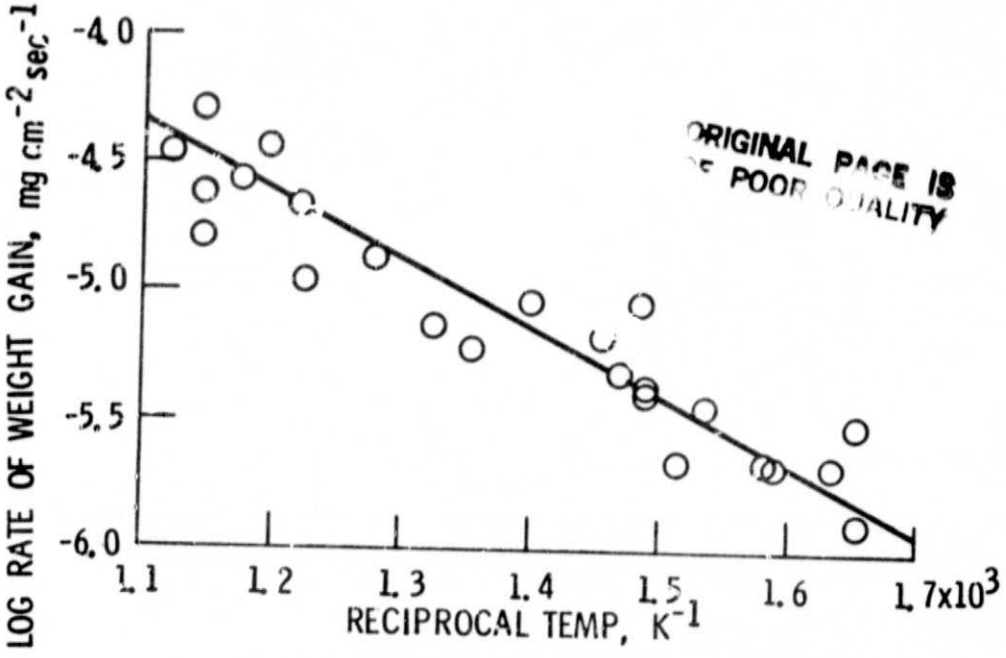

Figure 10
Thermogravimetric results for the conversion of single crystal NaCl to condensed Na_2SO_4 when 8 mole percent of SO_2 was added to flowing O_2 at atmospheric pressure.

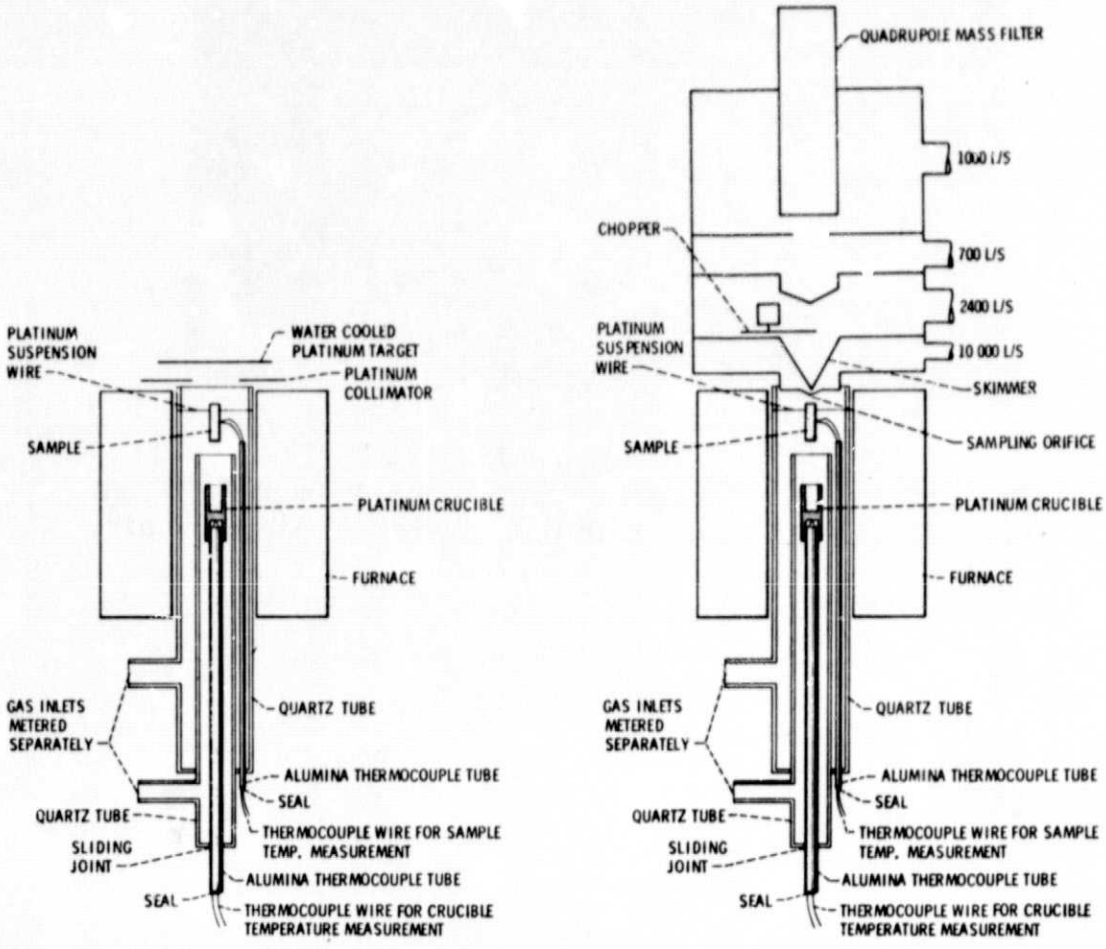

Figure 11
Schematic cross-section of target collection apparatus (left) and high pressure mass spectrometric sampler (right).

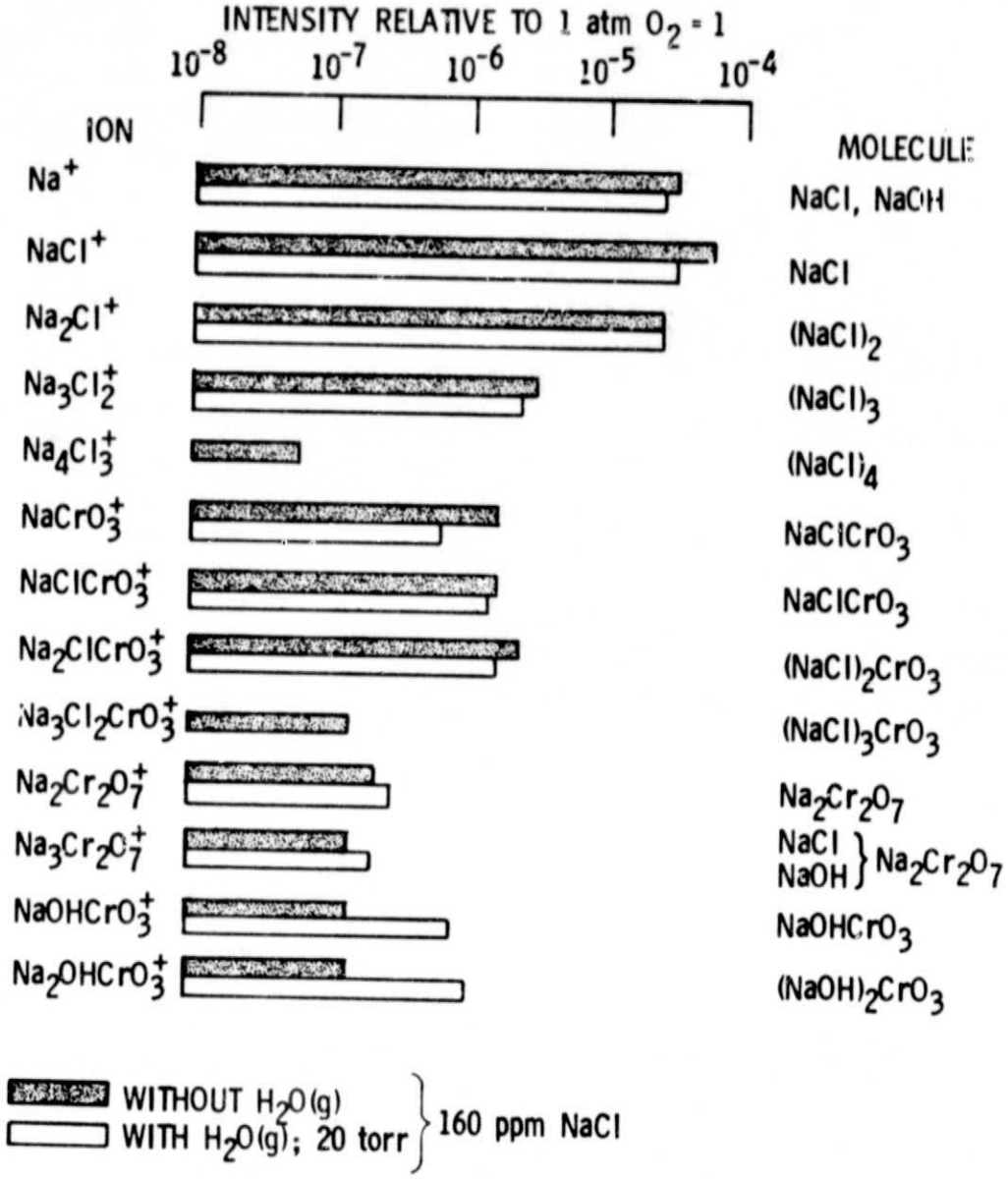

Figure 12
Mass spectrum of vapors over the Cr_2O_3(c) + O_2(g) + NaCl(g) system at 1020°C with and without added water vapor.

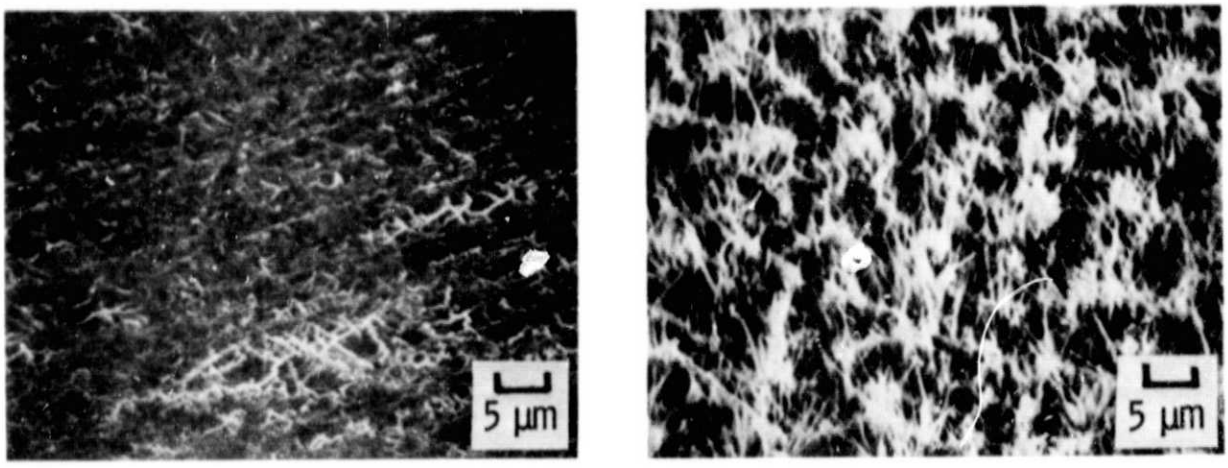

Figure 13
SEM micrographs of NiAl oxidized at 1050°C for 24 hours in air and in air with 10 ppm NaCl(g) added. From Ref. 11.

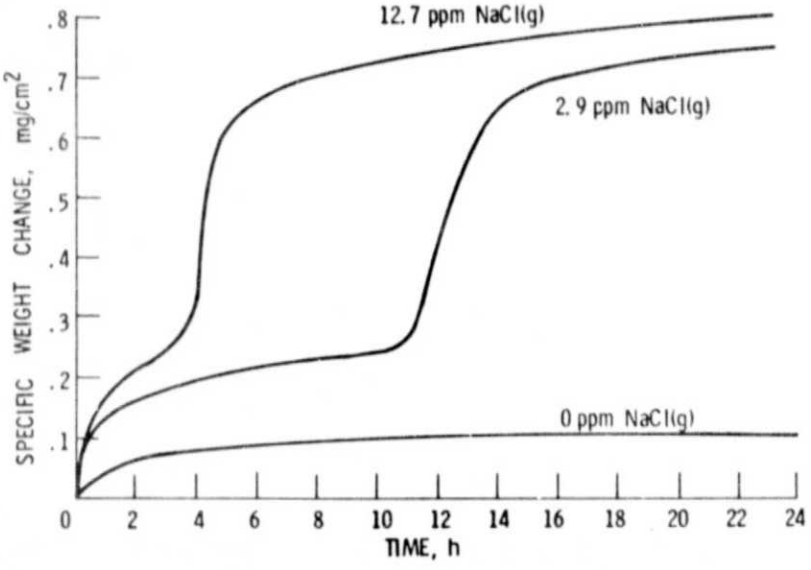

Figure 14
Thermogravimetric results for Ni25Cr oxidized at 900°C in air and in air with NaCl(g) added. From Ref. 11.